

Improving Single Injection CSF Delivery of AAV9-mediated Gene Therapy for SMA: A Dose–response Study in Mice and Nonhuman Primates

Kathrin Meyer¹, Laura Ferraiuolo¹, Leah Schmelzer¹, Lyndsey Braun¹, Vicki McGovern², Shibi Likhite^{1,3}, Olivia Michels¹, Alessandra Govoni¹, Julie Fitzgerald⁵, Pablo Morales⁴, Kevin D Foust⁵, Jerry R Mendell^{1,3,5}, Arthur HM Burghes² and Brian K Kaspar^{1,3,5}

¹The Research Institute at Nationwide Children's Hospital, Columbus, Ohio, USA; ²Department of Molecular & Cellular Biochemistry, The Ohio State University Medical Center, Columbus, Ohio, USA; ³Molecular, Cellular & Developmental Biology Graduate Program, The Ohio State University, Columbus, Ohio, USA; ⁴Mannheimer Foundation, Inc., Homestead, Florida, USA; ⁵Department of Neuroscience, The Ohio State University, Columbus, Ohio, USA

Spinal muscular atrophy (SMA) is the most frequent lethal genetic neurodegenerative disorder in infants. The disease is caused by low abundance of the survival of motor neuron (SMN) protein leading to motor neuron degeneration and progressive paralysis. We previously demonstrated that a single intravenous injection (IV) of self-complementary adeno-associated virus-9 carrying the human SMN cDNA (scAAV9-SMN) resulted in widespread transgene expression in spinal cord motor neurons in SMA mice as well as nonhuman primates and complete rescue of the disease phenotype in mice. Here, we evaluated the dosing and efficacy of scAAV9-SMN delivered directly to the cerebral spinal fluid (CSF) via single injection. We found widespread transgene expression throughout the spinal cord in mice and nonhuman primates when using a 10 times lower dose compared to the IV application. Interestingly, in nonhuman primates, lower doses than in mice can be used for similar motor neuron targeting efficiency. Moreover, the transduction efficacy is further improved when subjects are kept in the Trendelenburg position to facilitate spreading of the vector. We present a detailed analysis of transduction levels throughout the brain, brainstem, and spinal cord of nonhuman primates, providing new guidance for translation toward therapy for a wide range of neurodegenerative disorders.

Received 25 July 2014; accepted 24 October 2014; advance online publication 9 December 2014. doi:10.1038/mt.2014.210

INTRODUCTION

Spinal muscular atrophy (SMA) is a devastating disorder causing progressive skeletal muscle atrophy due to loss of α -motor neurons in the spinal cord.¹ It is the most common genetic cause of infant mortality in the United States.² The disease affects ~1

in 10,000 newborns^{3,4} and is categorized according to phenotypic severity, spanning type 0–IV.^{5,6} While type 0 represents the most severe form, displaying symptoms at birth, type I is the most frequent form, with signs of weakness arising before the age of 6 months. Types II–IV have a later onset and are milder. The motor neuron degeneration is caused by reduced abundance of the survival motor neuron protein (SMN), in the absence of a functional SMN1 gene. The low levels of SMN protein found in patients are produced by a nearly identical gene named SMN2.^{7,8} SMN2 harbors a silent mutation in exon 7 that alters the splicing of the mRNA leading to the predominant production of a truncated, unstable protein along with a minority of correctly spliced transcripts, generating low levels of full length protein.^{9–11} The copy number of SMN2 modifies disease severity, as gradually increased amounts of SMN protein become available in patients with more copies, resulting in milder SMA types II–IV.^{12,13} Since the level of SMN protein determines the severity of the disease, substantial effort has been put in the development of therapeutic strategies to improve SMN protein production by various methods, including small molecule-based drugs, SMN2 splicing correction, as well as overexpression of a human full-length SMN cDNA (reviewed in ref. 14). We and others have previously demonstrated that the expression of SMN via adeno-associated viral vectors is a very promising therapeutic strategy for SMA.^{15–20} In fact, a single intravenous injection (IV) of scAAV9 delivering SMN under the chicken- β -actin promoter (scAAV9.CBA.SMN) was sufficient to rescue the disease phenotype in the standard SMA mouse model, SMN Δ 7 (Smn $^{-/-}$, SMN2 $^{+/+}$, SMN Δ 7 $^{+/+}$) and increased the median survival from 15.5 days to more than 200 days.¹⁵ However, concerns remain that IV injections might not always be the best route to deliver therapeutic genes to the central nervous system (CNS) given the large amounts of vector required as well as the potential immunological response to peripheral transduction of other organs.^{21,22}

The first two authors are the first authors of this study.

Correspondence: Brian K Kaspar, The Research Institute at Nationwide Children's Hospital, 700 Children's Drive WA 3022, Columbus, Ohio 43205, USA. E-mail: Brian.Kaspar@NationwideChildrens.org

Recent work evaluated the potential of intramuscular or cerebral spinal fluid (CSF) delivery of AAV-SMN, with results ranging from mild to substantial increases in median survival up to 204 days in the SMNΔ7 mouse, depending on different dosing and injection protocols.^{18–20,23,24} Several studies quantified transduction levels and patterns in brain and spinal cord of mice after CSF and IV delivery of AAV.^{24–29} The use of different injection strategies, AAV serotypes, as well as dosing led to variable results in pigs and nonhuman primates.^{21,24,30–34} To determine the best injection method and to correctly estimate the effective dose needed in patients, an understanding of AAV transduction in brain and spinal cord in rodents and primates is required.^{21,35–37} This will elucidate how results obtained in rodents can be translated to primates. Therefore, in the present dose–response study, we first determined the minimally effective dose for increased survival using a single intracerebroventricular (ICV) injection of scAAV9.CBA.SMN in the most frequently used mouse model for SMA (SMNΔ7 mouse).³⁸ We found that the lowest dose leading to a significant and substantial increase in survival after a single ICV injection at postnatal day 1 was 1.8e13 vector genomes per kilogram (vg/kg). This minimally effective dosage led to a 165-day median survival in a mouse model that typically succumbs at 2 weeks of age. Increasing the dosage to 2.6e13 and 3.3e13 vg/kg resulted in median survival of 274 and 282 days, respectively. Of importance, ICV delivery demonstrated efficacy with a dose at least 10 times lower compared to IV injections¹⁵ that correlated to levels

of SMN mRNA found within the spinal cord. We determined that the minimal effective dosage resulted in ~20–40% of motor neurons targeted throughout the spinal cord. We next explored motor neuron targeting in nonhuman primates. Interestingly, motor neuron transduction was more efficient in nonhuman primates than in mice at a given dose. Moderate transduction was also seen in the motor cortex and cerebellum. Notably, we were able to further improve the transduction rate in the brain and brainstem when the nonhuman primates were kept in the Trendelenburg position for 5–10 minutes postinjection. These results highlight the potential of CSF delivery of AAV as a gene therapy approach for a wide range of neurodegenerative disorders, including SMA. Along with the presented detailed biodistribution including DNA and RNA data in nonhuman primates, this study sets the stage for initiating human clinical trials in SMA using a CSF route of dosing.

RESULTS

Single ICV injection of scAAV9.CBA.SMN increases survival of SMNΔ7 mice

In order to determine the minimally effective dose of scAAV9.CBA.SMN following single ICV injections, we performed a dose response of the vector into individual cohorts of 10–15 SMAΔ7 mice at postnatal day one (P1). Survival and weight gain was monitored daily and compared to the median survival of untreated SMAΔ7 mice (17.5 days). In order to facilitate the comparison to nonhuman primates, we measured all dosing in

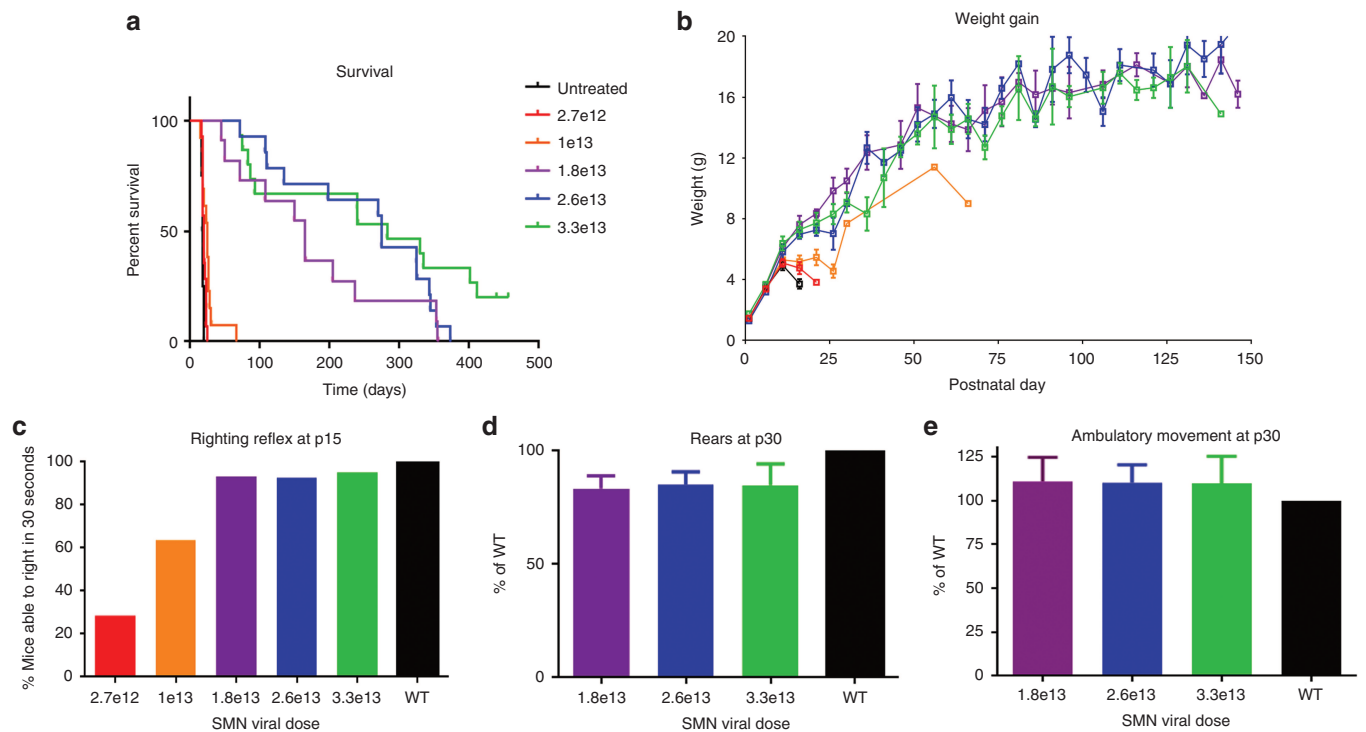


Figure 1 Single intracerebroventricular injections of scAAV9.CBA.SMN improve survival and motor performances of SMNΔ7 mice. **(a)** Five different doses of scAAV9.CBA.SMN were tested in SMNΔ7 mice. The first and second dose (2.7e12 and 1e13 vg/kg) led to no and very mild increase in survival respectively. With 1.8e13 vg/kg, survival significantly increased from 17.5 days in untreated mice to a median of 165 days (purple line, *P* value = 0.05). The two higher doses (2.6e13 and 3.3e13 vg/kg) led to a further increase in survival to a median of 274 and 282 days respectively (blue and green line, *P* values = 0.001 and 0.0001). **(b–e)** The increase in survival correlated with increase in weight and rescue of motor performances compared to wild type mice. Error bars = SEM; *n* = 10–15 per group.

vector genomes per kilogram (vg/kg). Since the average weight of the pups in our study was 1.51 g at P1 with a very small SEM of ± 0.1 , each pup was injected with the dose calculated for a 1.5 g pup. In our previous study, a single IV injection of 3.3×10^{14} vg/kg at P1 was sufficient to rescue the SMA phenotype in the SMA $\Delta 7$ mice. Based on this dose, we decided to start the ICV dose–response study with a 10 times lower dose at 3.3×10^{13} vg/kg and from there reduce the dose with four equal steps down to 2.7×10^{12} vg/kg, thereby covering lowest and highest doses previously used in a wide range of AAV CSF delivery studies in mice, pigs, and nonhuman primates. With the highest dose, 3.3×10^{13} vg/kg, we observed a dramatic, statistically significant effect on survival with a median of 282 days (P value = 0.0001 compared to untreated) and 1/3 of the animals surpassing 400 days at the time of the submission of this manuscript (Figure 1a). To our

knowledge, this is the highest increase in survival observed in this standard SMA animal model reported to date. Furthermore, with the next two lower doses (2.6×10^{13} and 1.8×10^{13} vg/kg), the median survival was still significantly increased to 274 days (P value = 0.001) and 165 days (P value = 0.05) respectively (Figure 1a). At a dose of 1×10^{13} or 2.7×10^{12} vg/kg, we observed median survivals of 24 and 19 days, which were not significantly different from the untreated control. However, with both low doses, we still observed a slightly better weight gain and an increase of 20 and 60% in the righting reflex at p15 compared to untreated (Figure 1b,c). The weight gain between the three higher doses was very similar and the righting reflex at p15 was almost completely restored. No differences were found in rear breaks or ambulatory movements at day 30 between groups receiving 1.8×10^{13} , 2.6×10^{13} , or 3.3×10^{13} vg/kg compared to wild-type

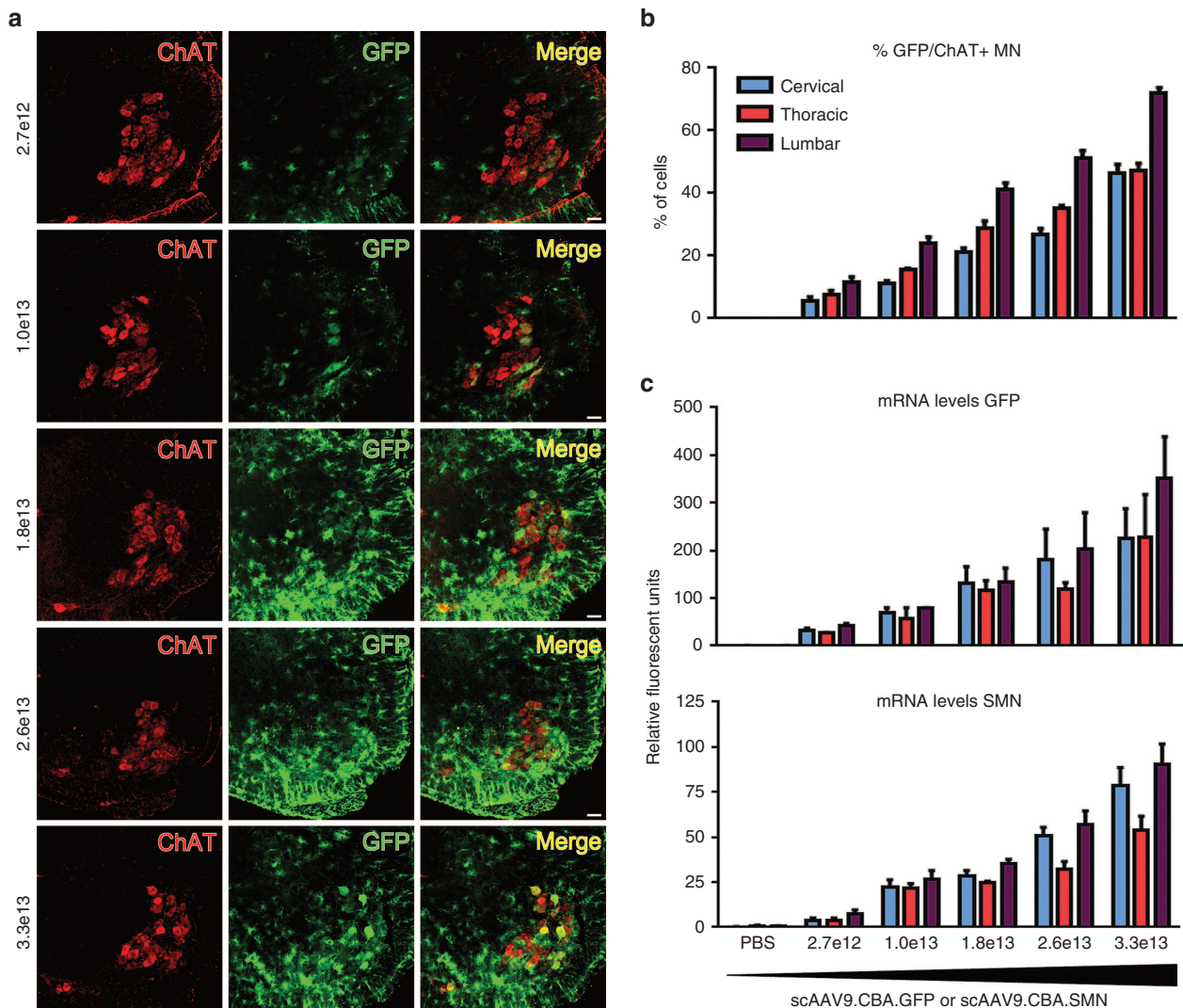


Figure 2 Single intracerebroventricular injections of scAAV9.CBA.GFP reveal that targeting 20–40% of the spinal motor neurons is required to achieve significant improvement in survival and motor performances of SMN $\Delta 7$ mice. **(a)** SMN $\Delta 7$ mice were injected with scAAV9.CBA.GFP using the same dosing regime as for SMN, immunofluorescence revealed increasing GFP levels with higher doses. **(b)** ChAT⁺/GFP⁺ cell counts revealed that the first dose leading to significant increase in survival corresponds to targeting of about 20–40% of spinal motor neurons. The highest most effective dose results in the targeting of about 46–72% of motor neurons. **(c)** GFP and SMN mRNA levels were measured in injected heterozygote littermates via digital droplet polymerase chain reaction. All samples were normalized to cyclophilin. The expression patterns of the two transcripts overlap and correlate with the increase in viral dose and motor neuron counts in all spinal cord segments. Error bars = SD; $n = 3$ per group.

animals (Figure 1d,e). The survival increase and behavioral benefits achieved with the doses 2.6e13 and 3.3e13 vg/kg were similar to what we previously observed with a ten times higher single IV injection (3.3e14 vg/kg).¹⁵ However, the highest dose seemed to have an additional benefit over 2.6e13 vg/kg since none of the animals in the second group surpassed 400 days of age. Taken together, the correlation between dose and survival increase is very close. Based on the statistical significance in survival increase as well as behavioral improvements, we determined the lowest effective dose that should translate into a substantial benefit for patients to be 1.8e13 vg/kg. For further functional analysis, three animals from the lowest effective dose group (1.8e13 vg/kg) were sacrificed at p165 for electrophysiological tests. The electrophysiological data were published earlier this year in *Annals of Clinical and Translational Neurology*.³⁹ Briefly, while untreated P15 SMNΔ7 mice showed altered compound muscle action potentials and motor unit number estimations, the values for the treated animals were similar to wild-type mice.³⁹ Importantly, untreated SMNΔ7 mice are not alive at P165 for direct comparison to treated animals. In summary, these results strongly underline the potential of CSF delivered scAAV9.CBA.SMN for clinical applications.

Targeting of ~20–40% of motor neurons throughout the spinal cord is required for significant improvement in survival

To determine the percentage of motor neurons targeted that correlated with the increased lifespan as well as to translate the dosing to nonhuman primates, we injected scAAV9 containing the green fluorescent protein (GFP) expressed under the same chicken-β-actin promoter as the previous SMN construct. We used heterozygote SMNΔ7 littermates and analyzed spinal cord sections for transgene expression by immunofluorescence and quantitative reverse transcription polymerase chain reaction (RT-PCR) 10 days postinjection (Figure 2a–c). We saw a clear correlation between the administered dose and GFP mRNA and protein abundance in cervical, thoracic, and lumbar spinal cord. The GFP expression is highly abundant in ChAT-positive motor neurons in the lumbar spinal cord, especially with the three higher doses that led to significantly increased survival (Figure 2a). Importantly, as previously observed with IV injections,^{15,40} the GFP expression is not exclusively found in motor neurons, but targets also other cell types. The percentage of GFP/ChAT double positive motor neurons was lowest in the cervical region and highest in the lumbar region of the spinal cord for

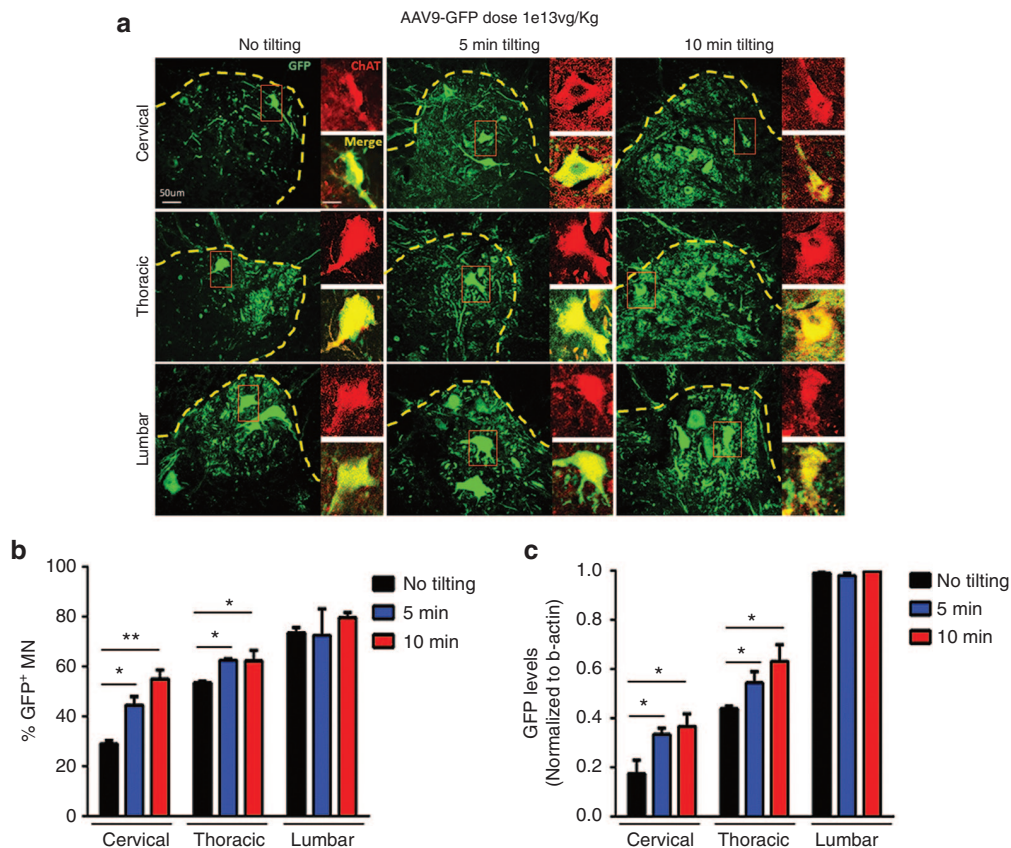


Figure 3 Single intrathecal sacral injection of 1e13 vg/kg scAAV9.CBA.GFP in nonhuman primates is sufficient to target >50% motor neurons in all spinal cord segments. **(a,b)** Seven cynomolgus macaques were injected with 1e13 vg/kg scAAV9.CBA.GFP via intrathecal sacral infusion. ChAT/GFP staining and cell counts of double positive cells reveal that keeping the subjects in the Trendelenburg position for 5 ($n = 2$) or 10 ($n = 3$) minutes significantly improves motor neuron transduction in both cervical and thoracic spinal cord compared to subjects that received standard procedure ($n = 2$). This procedure leads to targeting more than 50% motor neurons in all spinal cord segments. **(c)** GFP mRNA levels correlated with the increase in cell transduction and confirmed the positive effects of adopting the Trendelenburg position to improve virus distribution. Error bars = SD; $n = 2-3$ per group; * $P < 0.05$.

all doses (**Figure 2a,b**; **Supplementary Table S1**). At the lowest effective dose, we targeted 21% motor neurons in the cervical, 29% in the thoracic, and 41% in the lumbar region, while as for the highest dose, 46% cervical, 47% thoracic, and 72% lumbar motor neurons were GFP/ChAT double positive. Our findings closely match previous reports from other groups.²⁴ To further strengthen the immunofluorescence data, we measured the GFP mRNA levels by absolute quantitative droplet digital PCR. We found a similar dose-dependent increase with highest expression levels in the lumbar spinal cord regions in all cases (**Figure 2c**).

To ensure that GFP and SMN containing vectors have similar transduction patterns, we also injected heterozygote SMN Δ 7 littermates with scAAV9.CBA.SMN and equally analyzed these mRNA levels 10 days postinjection. The correlation between dose and increase in mRNA levels was similar between GFP and SMN transcripts for all doses and regions of the spinal cord (**Figure 2c**). In summary, our data suggest that targeting of at least 20–40% of motor neurons throughout the spinal cord should lead to a substantial therapeutic effect in patients, although a range closer \geq 50% would be preferable for maximum therapeutic benefit.

Lower doses lead to increased motor neuron transduction in nonhuman primates relative to mice

Based on our extensive experience with IV and CSF injections of scAAV9 constructs in pigs and nonhuman primates, we expected that the dose needed to achieve similar motor neuron transduction following CSF administration would be lower in nonhuman primates than in mice.^{21,40,41} Therefore, we injected two cynomolgus macaques with 1×10^{13} vg/kg scAAV9.CBA.GFP using a single intrathecal sacral infusion reflecting the preferred route for injection in SMA patients (**Supplementary Table S2**; **Supplementary Figure S1**). Two weeks following dosing, immunofluorescence staining and quantification revealed the abundance of GFP-positive cells throughout the spinal cord, with 73% of motor neurons targeted in the lumbar region, 53% of motor neurons targeted in thoracic region, and 29% in the cervical region (**Figure 3a,b**, black bars and **Supplementary Table S3**). These numbers confirmed our prediction, that nonhuman primate motor neuron targeting is improved compared to mouse studies. However, we next wished to explore whether we could improve the percentage of motor neurons targeted in the cervical and thoracic regions.

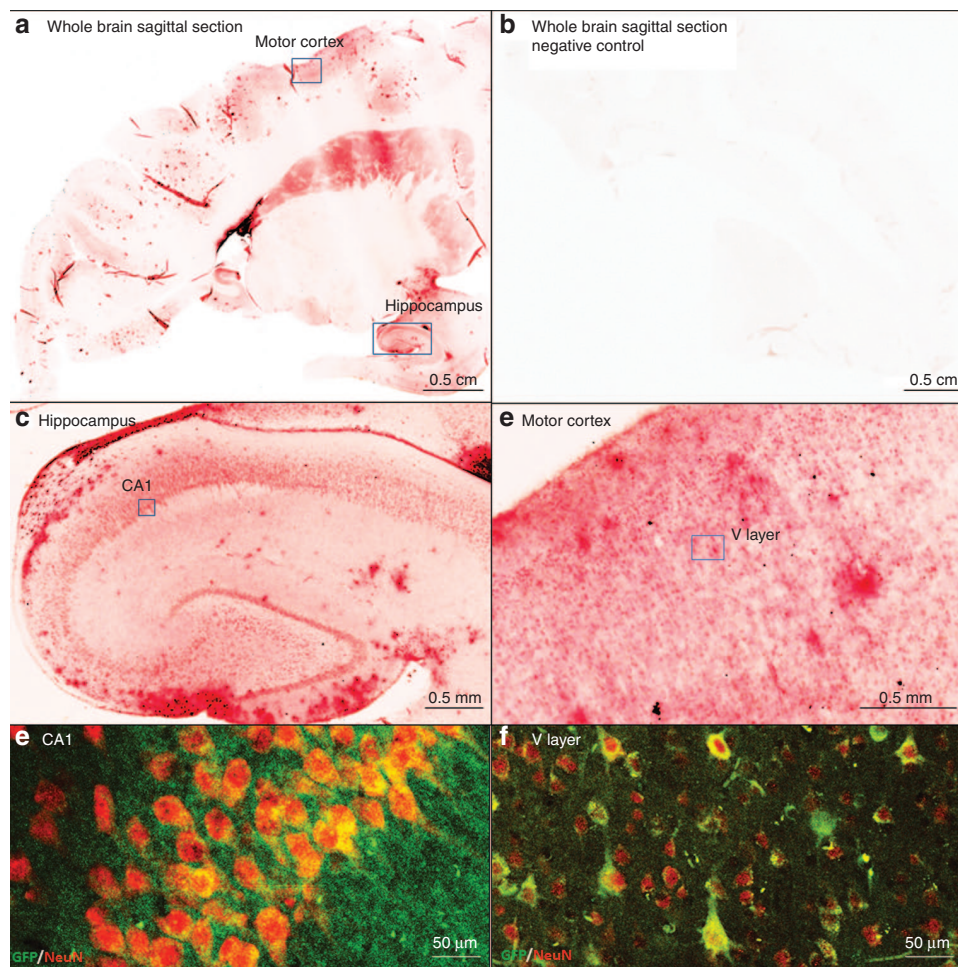


Figure 4 Wide cell transduction is achieved in the brain of nonhuman primates. **(a,b)** Wide cell transduction was achieved in several areas of the brain as shown by DAB staining **(a)** compared to the negative control **(b)**. **(c,d)** Among the regions with the highest transduction were hippocampus and motor cortex. **(e,f)** High-magnification pictures of CA1 neurons in the hippocampus and upper motor neurons in layer V of the motor cortex that are stained with GFP (green) and NeuN (red).

Improved transduction of the brain, cervical, and thoracic spinal cord is achieved when subjects are kept in the Trendelenburg position

Since SMA patients often die due to dysfunction of motor neurons that regulate respiration, it is imperative to improve targeting of upper spinal cord segments. A commonly used method to ensure proper spreading of small molecule drugs and anesthetics through the CSF is the Trendelenburg tilting table, on which the patient is tilted 15–30 degree head-down during drug infusion.⁴² In the attempt to optimize transduction levels of the upper spinal cord without increasing the vector dose, we applied the same technique to five cynomolgus macaques for 5 or 10 minutes after single intrathecal sacral injection of scAAV9.CBA.GFP (1e13 vg/kg) (Supplementary Table S2). Tilting the animals significantly improved transduction in the thoracic and cervical region of

the spinal cord, as demonstrated by immunofluorescence and quantification of GFP/ChAT double positive motor neurons (Figure 3a,b). Indeed, tilting for 10 minutes was sufficient to increase motor neuron transduction to 55, 62, and 80% in the cervical, thoracic, and lumbar region respectively (Supplementary Table S3), which implies major benefits for patients according to the rescue observed in the mouse model. The motor neuron counts tightly correlated with GFP transcript quantification in each of the spinal cord segments (Figure 3c).

Next, we analyzed the GFP expression throughout different brain and brainstem regions of the nonhuman primates that were kept in the Trendelenburg position (Figures 4 and 5). We found GFP in all brain regions (Figure 4a,b), with particularly strong signals in the hippocampus and in the motor cortex (Figure 4c–f). In the brainstem, several motor nuclei were highly transduced

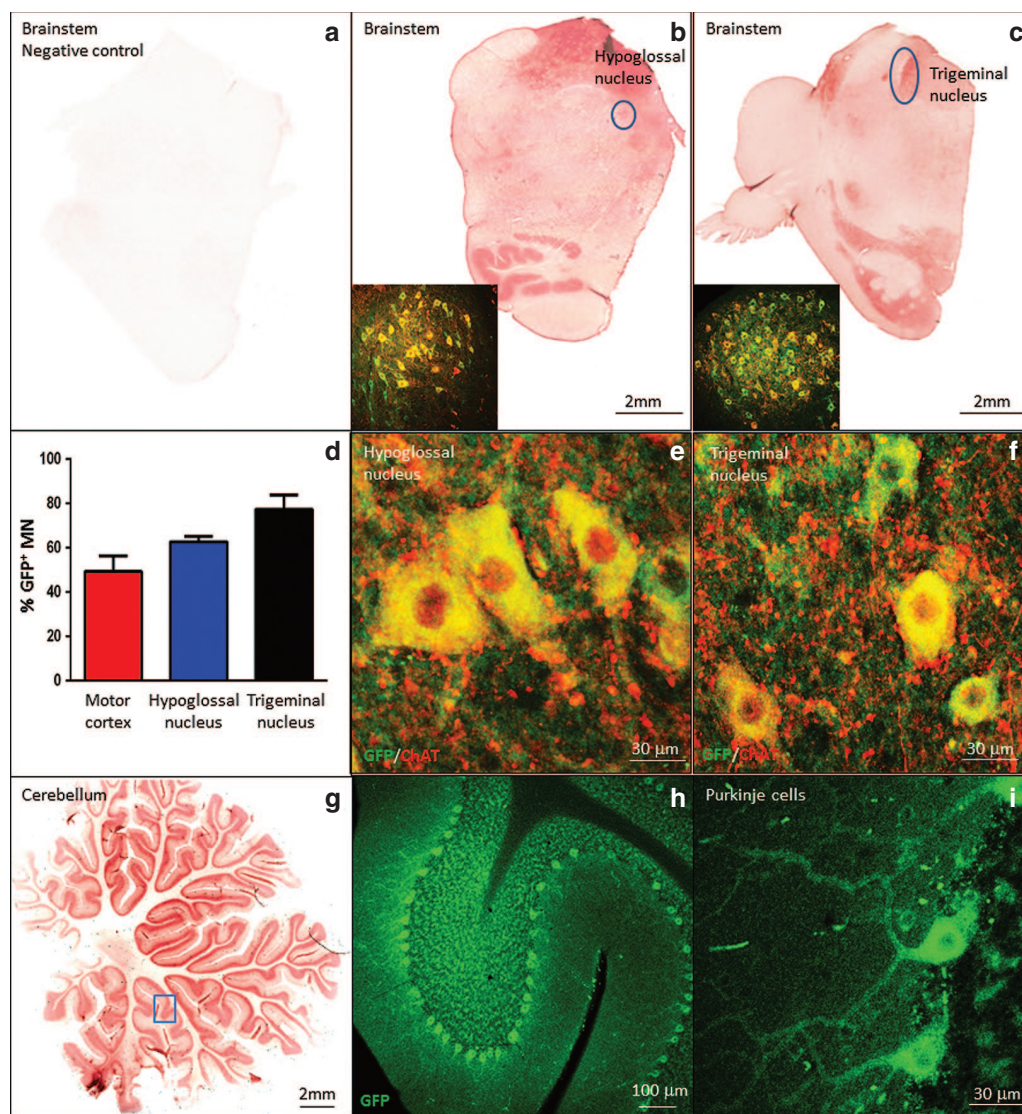


Figure 5 Wide cell transduction is achieved in the brain stem and cerebellum of nonhuman primates that were kept in the Trendelenburg position for 5 or 10 minutes. (a–f) DAB staining showed that several areas of the brainstem were transduced by scAAV9.CBA.GFP compared to the negative control (a–c). In particular, the XII and the V cranial nerve nuclei, the hypoglossal (b–e) and the trigeminal (c–f) nucleus respectively, were highly targeted. (d) Upper motor neuron counts revealed that about 50% motor neurons were transduced in the V layer of the motor cortex, and more than 60 and 75% motor neurons were GFP⁺ in the hypoglossal and trigeminal nucleus respectively; GFP (green) and ChAT (red). (g–i) High transduction levels were also achieved in the cerebellum, in particular the Purkinje cells and the nuclear layer. Error bars = SD; *n* = 5.

(Figure 5a–c), in particular, the hypoglossal and trigeminal nuclei, with more than 60 and 75% GFP⁺/Chat⁺ motor neurons respectively (Figure 5d–f and Supplementary Table S4). These nuclei are responsible for motor functions such as swallowing, speech, and facial expressions. In the cerebellum, both Purkinje cells and cells of the nuclear layer demonstrated high GFP expression levels (Figure 5g–i). In summary, the tilting had a major impact on the transduction efficiency in the brain, a finding that will likely facilitate gene therapeutic approaches for several neurodegenerative disorders like Rett syndrome and amyotrophic lateral sclerosis.^{43,44}

Detailed DNA and RNA biodistribution analyses reveal targeting of CNS and peripheral organs

To determine whether CSF delivery can reduce the transduction of peripheral organs compared to the IV injections, we performed a detailed biodistribution analysis on the tissue of the nonhuman primates that were placed head down in the Trendelenburg position for either 5 or 10 minutes ($n = 5$). These animals were selected over the nonhuman primates that were not placed head down because the treatment highly improved distribution in the spinal cord and brain, favoring this approach for clinical trials. Two weeks postinjection, the cynomolgus macaques were sacrificed and various tissues were collected to perform detailed DNA and RNA biodistribution analyses (Figure 6). scAAV9.CBA.GFP was lower in most peripheral tissues except spleen and liver compared to the high levels in brain and spinal cord. These findings are in line with previous reports from other groups.^{30,31} Interestingly, in the skeletal muscles and the CNS, there is a strong correlation between DNA and RNA levels (Figure 6, black and white solid bars), while in soft tissues and glands, RNA levels are generally lower than expected for the viral genomes detected. In particular, testes, intestines, and spleen show a 1,000 times fewer RNA molecules than DNA. Despite the detection of AAV in peripheral organs, which is confirmed by us and others,^{30,31} there was a significant decrease in the amount of vector detected peripherally compared to systemic injection. Additionally, similar observations

were made when comparing mice that were injected either IV or ICV at P1 24 weeks post-treatment (Supplementary Figure S2). Thus, CSF delivery is adding a significant potential safety component to future clinical trials treating CNS disorders.

DISCUSSION

SMA currently remains a life-threatening condition leading to paralysis, muscle atrophy, and eventually death. Although major progress has been made in patient care and support for breathing and nutrition, no treatment is available that halts or delays the degeneration of motor neurons and the connected muscular function. However, since the disease is caused by low amounts of SMN protein, several promising approaches are currently in pre-clinical and clinical trials aiming to increase SMN production.^{45,46} Gene therapy is a promising approach to achieve this goal and is appealing due to the long-lasting effects of a single administration. Several research teams, including ours, have demonstrated that single IV injections of self-complementary AAV9-SMN can drastically alter disease progression in the most frequently used SMA mouse model (SMNΔ7 mouse) and improve survival from 15 days to greater than 200 days.^{15,18,24} Indeed, this approach is currently in a phase 1/2 human clinical trial for SMA type 1 infants. More efficient delivery to spinal motor neurons could improve on these results for several reasons: (i) the amount of vector required for human clinical trials may be drastically reduced, which lowers the production and treatment cost, allowing inclusion of larger groups of patients as well as older individuals (SMA type II and III). (ii) The risk of potential side effects is likely lower since peripheral organs are less exposed to high amounts of the vector. (iii) Circulating antibodies neutralizing the therapeutic vector may be avoided by injecting directly into the CSF, which could help to improve efficacy in antibody-positive patients. (iv) The dose could be increased in very severe patients by combining IV and CSF administration if needed.

To date, few studies have evaluated the transduction pattern of scAAV9 delivered transgenes in the CNS of larger animal species

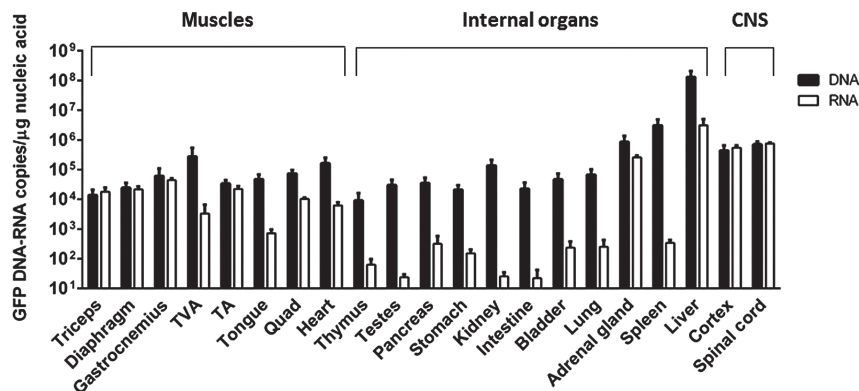


Figure 6 DNA and RNA biodistribution in nonhuman primates 2 weeks postinjection. DNA and RNA were isolated from 1 mg tissue biopsies and tested for the presence of viral genome as well as GFP mRNA molecules. Biodistribution comparison was achieved by interpolating Taqman quantitative polymerase chain reaction (qPCR) values for viral DNA or RNA to the same standard curve obtained with serial dilutions of the same plasmid carrying GFP and its CBA promoter. DNA biodistribution showed the presence of scAAV9.CBA.GFP (expressed as viral genome molecules/μg of total extracted DNA) at high levels in the targeted tissues, brain and spinal cord, as well as muscles and peripheral organs. RNA biodistribution revealed that GFP expression (expressed as GFP mRNA molecules/μg of total extracted RNA) differs significantly among different organs and tissues. The comparison shows that a close correlation exists between DNA and RNA levels in the central nervous system and in muscles; however, RNA levels are significantly lower in internal organs, apart from liver and adrenal glands.

after direct CSF delivery.^{21,24,34,47} Furthermore, the use of different AAV serotypes, different promoters, as well as multiple injection sites and routes (IV versus cisterna magna versus lumbar puncture) make comparisons and straight forward conclusions for application in clinical trials difficult. In this current study, we used the same vector from our previous studies of IV injections in mice and nonhuman primates. Our aim was to specifically determine the optimal dose for future clinical trials in human patients in a systematic manner. Therefore, we first determined the minimal effective dose leading to a 10-fold increase in survival of SMN Δ 7 mice with a single ICV injection at postnatal day 1 of scAAV9.CBA.SMN (1.8e13 vg/kg, median survival 165 days). Interestingly, 3.3e13 vg/kg, which is nearly twice as much vector, led to nearly a doubling of the median survival from 165 to 282 days, indicating a strong correlation between vector amount and increase in survival. Furthermore, by using a 10 times lower dosage compared to our previous IV study (3e14 vg/kg),¹⁵ we achieved the highest improvement in survival reported to date in this severe SMA mouse model.

To determine the percentage of motor neurons targeted with different doses, we used the same vector expressing GFP under the same CBA promoter. Since the transcription efficiency and therefore the expression profiles of cell types change depending on the promoter used,^{28,30} an accurate comparison is only possible using the same promoter. We see a strong correlation between GFP mRNA levels and the corresponding protein levels observed by immunofluorescence. Both, the GFP mRNA levels as well as the percentage GFP/ChAT positive motor neurons is highest in the lumbar spinal cord, which is consistent with previous reports from other groups.^{31,34} The dose response of the mRNA levels was very similar between the scAAV9.CBA.SMN and scAAV9.CBA.GFP, indicating that GFP can be used to approximate SMN expression patterns when using the same promoter. The minimal percentage of targeted motor neurons required for a clinically meaningful effect of survival in mice is ~21% in the cervical region, 29% in the thoracic, and 41% in the lumbar spinal cord, a finding that confirms previous observations in SMA mice.²⁴ With 3.3e13 vg/kg, our highest dose, we reached 46, 47, and 72% of spinal motor neurons in the cervical, thoracic, and lumbar regions respectively. It is interesting that several groups reported that the level of transduction remains highest in the lumbar region, although in these studies the injection was performed ICV or via Cisterna Magna.³¹ The reason for this phenomenon is currently unclear, but several aspects, such as differential expression of receptors, the flow of the CSF, or the larger area of nerve roots in contact with CSF in the lumbar region, could play a role.

We applied the knowledge from the ICV mouse studies and our previous IV studies in nonhuman primates²¹ to determine the dose range for the CSF delivery in macaque. Again, a 30 times lower dose compared to the previous systemic delivery (1e13 versus 3.3e14 vg/kg) injected via single sacral injection was sufficient to reach motor neuron transduction levels that may be clinically meaningful in SMA patients (29% cervical, 53% thoracic, and 73% lumbar). Strikingly, the transduction rate with the same dose was drastically improved when subjects were kept in the Trendelenburg position for 10 minutes after vector infusion, targeting 55, 62, and 80% of motor neurons

in the cervical, thoracic, and lumbar spinal cord respectively. The beneficial effect of tilting was highest in the brain and cervical region and less profound closer to the lumbar injection site, indicating that the tilting improved the spreading of the vector through the spinal cord away from the injection site. Tilting tables are regularly used to spread intrathecal delivered anesthetics and drugs in adults and this study is the first one to demonstrate a similar effect on viral vector distribution.⁴² The improved transduction of cervical spinal cord regions, brainstem, and motor cortex in the brain is of major interest for SMA patients since these regions control muscles involved in all voluntary movements as well as breathing and swallowing. In addition, immunofluorescence and 3,3'-Diaminobenzidine (DAB) staining revealed a broad targeting of various brain regions such as brain cortex, hippocampus, cerebellum and several motor nuclei in the brain stem. Robust brain transduction is relevant for other neurological disorders that are candidates for gene therapy such as Rett syndrome, Alzheimer's disease, and amyotrophic lateral sclerosis. Our biodistribution data from nonhuman primates are in line with previous studies demonstrating lower transduction rates of peripheral organs with CSF delivery compared to systemic applications.^{26,31} CSF delivery resulted in use of lower viral doses and less peripheral organ transduction without compromising motor neuron targeting in the spinal cord. This approach indeed adds safety advantages from an immunological perspective, which remains a significant area of intense research and clinical interest. In addition, the detailed study of mRNA abundance in peripheral organs revealed that DNA distribution is not necessarily correlating with transgene expression. Especially, in spleen, lung, kidney, intestine, thymus, and testes, the mRNA was hardly detectable. It is not uncommon to observe variable activity of ubiquitous promoters among different tissues, which is likely the cause of the observed differences.^{30,48} Overall, apart from adrenal gland and liver, the mRNA levels are very low in the peripheral organs except muscle tissue. Expression in muscle could be advantageous especially for SMA, since several studies suggest the involvement of muscle to the disease phenotype.^{49,50}

In summary, our preclinical studies in mice with ICV delivery of scAAV9.CBA.SMN demonstrate unsurpassed survival in the mouse model of SMA. We provide strong evidence that CSF delivery of scAAV9.CBA.GFP combined with tilting leads to widespread transduction in the brain and spinal cord of nonhuman primates. Furthermore, 30 times lower doses compared to IV injections lead to transduction of up to 55–80% motor neurons in all regions of the spinal cord of nonhuman primates with this new injection route that includes tilting. Therefore, our study offers insight in vector distribution and its correlation with transgene expression and provides guidance for future AAV9-based clinical trials in SMA, as well as other neurodegenerative disorders.

MATERIALS AND METHODS

Animals. All procedures performed were in accordance with the National Institutes of Health guidelines and approved by the Research Institute at Nationwide Children's Hospital (Columbus, OH), or Mannheimer Foundation (Homestead, FL) Institutional Animal Care and Use Committees.

Mice. SMN Δ 7 mice were bred and genotyped as described previously. The primer sequences used were mouse Smn allele: forward 1: 5'-TCCAGCTCCGGGATATTGGGATTG, reverse 1: 5'-AGTCCCACCACCTAAGAAAGCC, forward 2: 5'-GTCTGGGCTGTAGGCATTGC, reverse 2: 5'-GCTGTGCCTTTTGGCTTATCTG), and mouse Smn knockout allele: forward: 5'-GCCTGCGATGTCGGTTTCTGTGAGG, reverse: 5'-CCAGCGCGGATCGGTCAGACG).

After analysis of the genotyping PCR, litters were culled to five animals. Affected animals or heterozygote littermates (Smn $^{-/-}$, SMN2 $+/+$, SMN Δ 7 $+/+$ or Smn $^{-/+}$, SMN2 $+/+$, SMN Δ 7 $+/+$) were injected with the different doses of scAAV9.CBA.SMN or scAAV9.CBA.GFP diluted in phosphate-buffered saline.

Behavior. Mice were monitored daily for survival and weight gain. At P15, they were tested for righting reflex by determining their ability to right themselves within 30 seconds after being put on their side. At P30, animals were tested in an open field analysis (San Diego Instruments, San Diego, CA). Animals were given several minutes to adapt within the testing chamber before the beginning of testing, then activity was monitored for 5 minutes. Beam breaks were recorded in the x, y, and z planes and averaged across groups.

Monkeys. Adult, 1-year-old cynomolgus macaques (*Macaca fascicularis*) with average body weight of 2 kg were used for this study at the Mannheimer Foundation. Regular monitoring of overall health and body weight was performed prior and after the injections to assess the welfare of the animals.

Injections. For ICV injections of mice at P1, the pups were anesthetized on ice for 10 minutes prior to injection. Injection was performed with laser-pulled borosilicate glass needles (Sutter Instruments, Novato, CA, O.D.: 1.2 mm, I.D.: 0.69 mm 10 cm length) as previously described.^{51,52} The AAV9 vectors were diluted in phosphate-buffered saline for lower doses. The total volume injected for each animal was 5 μ l.

For IV injections, newborn mice were injected with 3.3e14 vg/kg in a total volume of 50 μ l as previously described.^{15,41} Of note, this dose leads to equivalent improvement in survival compared to ICV 3.3e13 vg/kg3.

For nonhuman primate injections, anesthetized cynomolgus monkeys ($n = 7$) received intrathecal injections of 1×10^{13} vg/kg scAAV9-GFP. The injection was performed by lumbar puncture into the subarachnoid space of the lumbar thecal sac. AAV9-GFP was resuspended with omnipaque (iohexol), an iodinated compound routinely used in the clinical setting. Iohexol is used to validate successful subarachnoid space cannulation and was administered in the dose of 100 mg/kg. The subject was placed in the lateral decubitus position and the posterior midline injection site at ~L4/5 level identified (below the conus of the spinal cord). Under sterile conditions, a spinal needle with stylet was inserted and subarachnoid cannulation was confirmed with the flow of clear CSF from the needle. 0.8 ml of CSF was drained in order to decrease the pressure in the subarachnoid space and immediately after 100 mg/kg iohexol mixed with 1×10^{13} vg/kg scAAV9-GFP was injected. Five of the seven subjects that underwent the procedure were kept in the Trendelenburg position and their body was tilted head-down for either 5 ($n = 2$) or 10 ($n = 3$) minutes.

Perfusion and tissue processing. Mice were sacrificed at P10 for immunofluorescence analysis. Animals were anesthetized with xylazine/ketamine cocktail, followed by cervical dislocation and tissue dissection. Tissue pieces were incubated in 4% paraformaldehyde overnight. Following cryoprotection with 30% sucrose, spinal cords were frozen in isopentane at -65°C , and serial 40- μm sections were collected free floating using a sliding microtome. Serial sections were kept in a 96-well plate that contained 4% paraformaldehyde and were stored at 4°C .

Cynomolgus monkeys injected with virus were euthanized 2 weeks postinjection. Animals were anesthetized with sodium pentobarbital at

the dose of 80–100 mg/kg IV and perfused with saline solution. Brain and spinal cord dissection were performed immediately and tissues were processed either for nucleic acid isolation (snap frozen) or postfixed in 4% paraformaldehyde and subsequently cryoprotected with 30% sucrose and frozen in isopentane at -65°C .

Nonhuman primate spinal cords were sectioned using the cryostat. Fifteen-micrometer coronal sections were collected from cervical, thoracic, and lumbar cord for free floating immunostaining. Brains were sectioned using the microtome. Forty-micrometer coronal or sagittal sections were collected from brain, brainstem, and cerebellum for free floating immunostaining.

Immunohistochemistry. Both, mouse and monkey tissues were washed three-times for 10 minutes each in Tris-buffered saline (TBS), then blocked in a solution containing 10% donkey serum, 1% Triton X-100 and 1% penicillin/streptomycin for 2 hours at room temperature. All the antibodies were diluted with the blocking solution. Primary antibodies used were as follows: Ck Anti-GFP at 1:500 (Abcam, Cambridge, MA), Rb Anti-GFAP at 1:500 (Dako), and Gt Anti-ChAT at 1:50 (Millipore, Billerica, MA) for mouse and rabbit anti-GFP (1:400, Invitrogen, Carlsbad, CA), goat anti-ChAT (1:50, Millipore) and mouse anti-NeuN (1:100, Millipore) for monkey. Tissues were incubated in primary antibody at 4°C for 24–48 hours, then washed three times with TBS. After washing, tissues were incubated for 2 hours at room temperature in the appropriate fluorescein isothiocyanate (FITC)-, Cy3-, or Cy5-conjugated secondary antibodies (1:200, Jackson ImmunoResearch, Westgrove, PA) and DAPI (1:1,000, Invitrogen). Tissues were then washed three times with TBS, mounted onto slides, then coverslipped with PVA-DABCO. All images were captured on a Zeiss-laser-scanning confocal microscope.

For DAB staining, monkey spinal cord and brain sections were washed three times in TBS, blocked for 2 hours at RT in 10% donkey serum and 1% Triton X-100. Sections were then incubated overnight at 4°C with rabbit anti-GFP primary antibody (1:1,000, Invitrogen) diluted in blocking buffer. The following day, tissues were washed with TBS three times, incubated with biotinylated secondary antibody anti-rabbit (1:200, Jackson ImmunoResearch) in blocking buffer for 30 minutes at RT, washed three times in TBS, and incubated for 30 minutes at RT with ABC (Vector, Burlingame, CA). Sections were then washed for three times in TBS and incubated for 2 minutes with DAB solution at RT and washed with distilled water. These were then mounted onto slides and covered with coverslips in mounting medium. All images were captured with the Zeiss Axioscope.

Motor neuron quantification. Serial 12- μm -thick spinal cord sections, each separated by 60 μm , were labeled as described for GFP and ChAT expression. Fifteen stained sections per spinal cord segment per animal were serially mounted on slides from rostral to caudal, then coverslipped. Sections were evaluated using confocal microscopy (Zeiss) with a 40 \times objective and simultaneous FITC and Cy3 filters. The total number of ChAT-positive cells found in the ventral horns with defined soma was identified and GFP-labeled cells were quantified while checking for colocalization with ChAT.

As for the nonhuman primate brain and the brainstem, 40- μm -thick sections, each separated by 40 μm , were labeled as described for GFP and ChAT or NeuN (in the cortex) expression. Motor neuron counts of the V and XII cranial nerve were performed on the whole area covered by the motor nuclei, seven sections were examined for the motor neuron counts in the V layer of the motor cortex. The V layer of the motor cortex was identified following cortical structural parameters.

Droplet digital PCR. RNA from different segments of the mouse spinal cord was isolated using the RNeasy Mini kit (Qiagen, Valencia, CA). RNA was then reverse-transcribed into cDNA using the RT2 HT First Strand Kit (SABiosciences, Valencia, CA). Droplet digital PCR (ddPCR) was performed on DNase treated mouse spinal cord cDNA.

GFP was detected with FP 5'-CCACTACTGAGCACCCAGTC, RP 5'-TCCAGCAGGACCATGTGATC and probe FAM-TGAGCAAAGACC CCAACGAGAAGCG. AAV9:SMN expression was detected with AAV9 FP 5'-AATTCCTCCGGGATATCGTC, SMN RP 5'-gcgccggaacagcagcgaat, AAV9:SMN probe FAM-acgcgtccggccccacgct. This primer set is specific to SMN expression from the CBA promoter from the AAV9 vector. The primers do not amplify SMN from the SMN2 gene. Mouse cyclophilin was detected with FP 5'-gtcaacccaccgtgtcttct, RP 5'-ttggaacttctgtctgcaaca, and probe VIC-cttggccgctct. Droplet generation and reader analysis were performed on the QX100 (Bio-Rad). 15,000 to 18,000 droplets containing cDNA, primers, probe, 2× ddPCR SuperMix for Probes, and droplet generation oil were generated and amplified. A sufficient number of positive and negative droplets were read by the QX100 reader and quantified using the QuantaSoft software (Bio-Rad, Hercules, CA). The concentration of transcripts was determined using Poisson statistical distributions and relative GFP or AAV:SMN levels were determined by normalizing to mouse cyclophilin expression. Two technical replicates (for a total of >20,000 droplet PCR reactions) and three biological replicates were performed for each sample.

GFP qRT-PCR. RNA from different segments of the nonhuman primate spinal cord was isolated using the RNeasy Mini kit (Qiagen). RNA was then reverse-transcribed into cDNA using the RT2 HT First Strand Kit (SABiosciences). 12.5 ng RNA were used in each Q-PCR reaction using SyBR Green (Invitrogen) to establish the relative quantity of GFP transcript. Each sample was run in triplicate and relative concentration calculated using the ddCt values normalized to endogenous actin transcript.

Viral genome particles quantification. DNA and RNA were isolated from equal size 1 mg tissue biopsies from mouse and nonhuman primates using the QIAamp DNA Mini Kit and Trizol respectively. Nucleic acids for biodistribution were only isolated from the monkeys placed in the Trendelenburg position with head down for either 5 or 10 ($n = 5$). Absolute quantification of viral genome particles or GFP RNA molecules per μg of DNA or RNA was calculated interpolating the C_t values obtained with a standard curve ranging from 25 to 2×10^6 copies of viral plasmid.

Statistical analysis. All statistical tests were performed by one-way or two-way analysis of variance followed by a Bonferroni *post hoc* analysis of mean differences between groups (GraphPad Prism, San Diego, CA).

SUPPLEMENTARY MATERIAL

Figure S1. Representative myelogram obtained at time of intrathecal infusion of AAV9-GFP with iohexol.

Figure S2. Biodistribution comparing transgene levels in quadriceps, heart, lung and liver in mice ($n=3$ per group) 24 weeks after AAV9-SMN injection either via ICV or systemic delivery.

Table S1. Quantification of transduced motor neurons in mice treated with increasing doses of AAV9-SMN in the three segments of the spinal cord.

Table S2. Nonhuman primate age and weight details at time of infusion with AAV9-GFP and time spent in the Trendelenburg position.

Table S3. Quantification of transduced motor neurons in nonhuman primates in the three segments of the spinal cord.

Table S4. Quantification of transduced motor neurons in nonhuman primates in the three segments of the spinal cord.

ACKNOWLEDGMENTS

We are grateful from the support from National Institutes of Health/NINDS U01, Cure SMA, and The Sophia's Cure Foundation. L.F. is funded by the Marie Curie Fellowship. K.M. received a fellowship from the Swiss National Science Foundation. B.K.K. has intellectual property filed through Nationwide Children's Hospital, and an equity interest related to the work that is licensed to AveXis. B.K.K. also serves as a paid consultant for AveXis and serves on the AveXis Board of Directors. The various relationships are managed through a conflict management plan at The Research Institute at Nationwide Children's Hospital.

REFERENCES

- Crawford, TO and Pardo, CA (1996). The neurobiology of childhood spinal muscular atrophy. *Neurobiol Dis* **3**: 97–110.
- Roberts, DF, Chavez, J and Court, SD (1970). The genetic component in child mortality. *Arch Dis Child* **45**: 33–38.
- Pearn, J (1978). Incidence, prevalence, and gene frequency studies of chronic childhood spinal muscular atrophy. *J Med Genet* **15**: 409–413.
- Prior, TW, Snyder, PJ, Rink, BD, Pearl, DK, Pyatt, RE, Mihal, DC *et al.* (2010). Newborn and carrier screening for spinal muscular atrophy. *Am J Med Genet A* **152A**: 1608–1616.
- Zerres, K and Rudnik-Schöneborn, S (1995). Natural history in proximal spinal muscular atrophy. Clinical analysis of 445 patients and suggestions for a modification of existing classifications. *Arch Neurol* **52**: 518–523.
- Russman, BS (2007). Spinal muscular atrophy: clinical classification and disease heterogeneity. *J Child Neurol* **22**: 946–951.
- Lefebvre, S, Burlet, P, Liu, Q, Bertrand, S, Clermont, O, Munnich, A *et al.* (1997). Correlation between severity and SMN protein level in spinal muscular atrophy. *Nat Genet* **16**: 265–269.
- Coovert, DD, Le, TT, McAndrew, PE, Strasswimmer, J, Crawford, TO, Mendell, JR *et al.* (1997). The survival motor neuron protein in spinal muscular atrophy. *Hum Mol Genet* **6**: 1205–1214.
- Monani, UR, Lorson, CL, Parsons, DW, Prior, TW, Androphy, EJ, Burghes, AH *et al.* (1999). A single nucleotide difference that alters splicing patterns distinguishes the SMA gene SMN1 from the copy gene SMN2. *Hum Mol Genet* **8**: 1177–1183.
- Lorson, CL, Strasswimmer, J, Yao, JM, Baleja, JD, Hahnen, E, Wirth, B *et al.* (1998). SMN oligomerization defect correlates with spinal muscular atrophy severity. *Nat Genet* **19**: 63–66.
- Burnett, BG, Muñoz, E, Tandon, A, Kwon, DY, Sumner, CJ and Fischbeck, KH (2009). Regulation of SMN protein stability. *Mol Cell Biol* **29**: 1107–1115.
- Mailman, MD, Heinz, JW, Papp, AC, Snyder, PJ, Sedra, MS, Wirth, B *et al.* (2002). Molecular analysis of spinal muscular atrophy and modification of the phenotype by SMN2. *Genet Med* **4**: 20–26.
- McAndrew, PE, Parsons, DW, Simard, LR, Rochette, C, Ray, PN, Mendell, JR *et al.* (1997). Identification of proximal spinal muscular atrophy carriers and patients by analysis of SMN1 and SMN2 copy number. *Am J Hum Genet* **60**: 1411–1422.
- Arnold, WD and Burghes, AH (2013). Spinal muscular atrophy: development and implementation of potential treatments. *Ann Neurol* **74**: 348–362.
- Foust, KD, Wang, X, McGovern, VL, Braun, L, Bevan, AK, Haidet, AM *et al.* (2010). Rescue of the spinal muscular atrophy phenotype in a mouse model by early postnatal delivery of SMN. *Nat Biotechnol* **28**: 271–274.
- Valori, CF, Ning, K, Wyles, M, Mead, RJ, Grierson, AJ, Shaw, PJ *et al.* (2010). Systemic delivery of scAAV9 expressing SMN prolongs survival in a model of spinal muscular atrophy. *Sci Transl Med* **2**: 35ra42.
- Dominguez, E, Marais, T, Chatauret, N, Benkhelifa-Ziyyat, S, Duque, S, Ravassard, P *et al.* (2011). Intravenous scAAV9 delivery of a codon-optimized SMN1 sequence rescues SMA mice. *Hum Mol Genet* **20**: 681–693.
- Glascok, JJ, Shababi, M, Wetz, MJ, Krogman, MM and Lorson, CL (2012). Direct central nervous system delivery provides enhanced protection following vector mediated gene replacement in a severe model of spinal muscular atrophy. *Biochem Biophys Res Commun* **417**: 376–381.
- Benkhelifa-Ziyyat, S, Besse, A, Roda, M, Duque, S, Astord, S, Carcenac, R *et al.* (2013). Intramuscular scAAV9-SMN injection mediates widespread gene delivery to the spinal cord and decreases disease severity in SMA mice. *Mol Ther* **21**: 282–290.
- Passini, MA, Bu, J, Roskelley, EM, Richards, AM, Sardi, SP, O'Riordan, CR *et al.* (2010). CNS-targeted gene therapy improves survival and motor function in a mouse model of spinal muscular atrophy. *J Clin Invest* **120**: 1253–1264.
- Bevan, AK, Duque, S, Foust, KD, Morales, PR, Braun, L, Schmelzer, L *et al.* (2011). Systemic gene delivery in large species for targeting spinal cord, brain, and peripheral tissues for pediatric disorders. *Mol Ther* **19**: 1971–1980.
- Nathwani, AC, Tuddenham, EG, Rangarajan, S, Rosales, C, McIntosh, J, Linch, DC *et al.* (2011). Adenovirus-associated virus vector-mediated gene transfer in hemophilia B. *N Engl J Med* **365**: 2357–2365.
- Robbins, KL, Glascok, JJ, Osman, EY, Miller, MR and Lorson, CL (2014). Defining the therapeutic window in a severe animal model of spinal muscular atrophy. *Hum Mol Genet* **23**: 4559–4568.
- Passini, MA, Bu, J, Richards, AM, Treleaven, CM, Sullivan, JA, O'Riordan, CR *et al.* (2014). Translational fidelity of intrathecal delivery of self-complementary AAV9-survival motor neuron 1 for spinal muscular atrophy. *Hum Gene Ther* **25**: 619–630.
- Yang, B, Li, S, Wang, H, Guo, Y, Gessler, DJ, Cao, C *et al.* (2014). Global CNS transduction of adult mice by intravenously delivered rAAVrh.8 and rAAVrh.10 and nonhuman primates by rAAVrh.10. *Mol Ther* **22**: 1299–1309.
- Gray, SJ, Matagne, V, Bachaboina, L, Yadav, S, Ojeda, SR and Samulski, RJ (2011). Preclinical differences of intravascular AAV9 delivery to neurons and glia: a comparative study of adult mice and nonhuman primates. *Mol Ther* **19**: 1058–1069.
- Chakrabarty, P, Rosario, A, Cruz, P, Sieminski, Z, Ceballos-Diaz, C, Crosby, K *et al.* (2013). Capsid serotype and timing of injection determines AAV transduction in the neonatal mouse brain. *PLoS One* **8**: e67680.
- Gholizadeh, S, Tharmalingam, S, Macaladaz, ME and Hampson, DR (2013). Transduction of the central nervous system after intracerebroventricular injection of adeno-associated viral vectors in neonatal and juvenile mice. *Hum Gene Ther Methods* **24**: 205–213.
- Snyder, BR, Gray, SJ, Quach, ET, Huang, JW, Leung, CH, Samulski, RJ *et al.* (2011). Comparison of adeno-associated viral vector serotypes for spinal cord and motor neuron gene delivery. *Hum Gene Ther* **22**: 1129–1135.
- Dirren, E, Towne, CL, Setola, V, Redmond, DE Jr, Schneider, BL and Aebischer, P (2014). Intracerebroventricular injection of adeno-associated virus 6 and 9 vectors for cell type-specific transgene expression in the spinal cord. *Hum Gene Ther* **25**: 109–120.
- Gray, SJ, Nagabhushan Kalburgi, S, McCown, TJ and Jude Samulski, R (2013). Global CNS gene delivery and evasion of anti-AAV-neutralizing antibodies by intrathecal AAV administration in non-human primates. *Gene Ther* **20**: 450–459.

32. Federici, T, Taub, JS, Baum, GR, Gray, SJ, Grieger, JC, Matthews, KA *et al.* (2012). Robust spinal motor neuron transduction following intrathecal delivery of AAV9 in pigs. *Gene Ther* **19**: 852–859.
33. Samaranch, L, Salegio, EA, San Sebastian, W, Kells, AP, Foust, KD, Bringas, JR *et al.* (2012). Adeno-associated virus serotype 9 transduction in the central nervous system of nonhuman primates. *Hum Gene Ther* **23**: 382–389.
34. Samaranch, L, Salegio, EA, San Sebastian, W, Kells, AP, Bringas, JR, Forsayeth, J *et al.* (2013). Strong cortical and spinal cord transduction after AAV7 and AAV9 delivery into the cerebrospinal fluid of nonhuman primates. *Hum Gene Ther* **24**: 526–532.
35. Passini, MA, Watson, DJ, Vite, CH, Landsburg, DJ, Feigenbaum, AL and Wolfe, JH (2003). Intraventricular brain injection of adeno-associated virus type 1 (AAV1) in neonatal mice results in complementary patterns of neuronal transduction to AAV2 and total long-term correction of storage lesions in the brains of beta-glucuronidase-deficient mice. *J Virol* **77**: 7034–7040.
36. Cearley, CN, Vandenberghe, LH, Parente, MK, Carnish, ER, Wilson, JM and Wolfe, JH (2008). Expanded repertoire of AAV vector serotypes mediate unique patterns of transduction in mouse brain. *Mol Ther* **16**: 1710–1718.
37. Zhang, H, Yang, B, Mu, X, Ahmed, SS, Su, Q, He, R *et al.* (2011). Several rAAV vectors efficiently cross the blood-brain barrier and transduce neurons and astrocytes in the neonatal mouse central nervous system. *Mol Ther* **19**: 1440–1448.
38. Le, TT, Pham, LT, Butchbach, ME, Zhang, HL, Monani, UR, Covert, DD *et al.* (2005). SMN Δ 7, the major product of the centromeric survival motor neuron (SMN2) gene, extends survival in mice with spinal muscular atrophy and associates with full-length SMN. *Hum Mol Genet* **14**: 845–857.
39. Arnold, WD, Porensky, PN, McGovern, VL, Iyer, CC, Duque, S, Li, X *et al.* (2014). Electrophysiological Biomarkers in Spinal Muscular Atrophy: Preclinical Proof of Concept. *Ann Clin Transl Neurol* **1**: 34–44.
40. Foust, KD, Salazar, DL, Likhite, S, Ferraiuolo, L, Ditsworth, D, Ilieva, H *et al.* (2013). Therapeutic AAV9-mediated suppression of mutant SOD1 slows disease progression and extends survival in models of inherited ALS. *Mol Ther* **21**: 2148–2159.
41. Foust, KD, Nurre, E, Montgomery, CL, Hernandez, A, Chan, CM and Kaspar, BK (2009). Intravascular AAV9 preferentially targets neonatal neurons and adult astrocytes. *Nat Biotechnol* **27**: 59–65.
42. Setayesh, AR, Kholdebarin, AR, Moghadam, MS and Setayesh, HR (2001). The Trendelenburg position increases the spread and accelerates the onset of epidural anesthesia for Cesarean section. *Can J Anaesth* **48**: 890–893.
43. Garg, SK, Liou, DT, Cheval, H, McGann, JC, Bissonnette, JM, Murtha, MJ *et al.* (2013). Systemic delivery of MeCP2 rescues behavioral and cellular deficits in female mouse models of Rett syndrome. *J Neurosci* **33**: 13612–13620.
44. Braak, H, Brettschneider, J, Ludolph, AC, Lee, VM, Trojanowski, JQ and Del Tredici, K (2013). Amyotrophic lateral sclerosis—a model of corticofugal axonal spread. *Nat Rev Neurol* **9**: 708–714.
45. Osman, EY, Yen, PF and Lorson, CL (2012). Bifunctional RNAs targeting the intronic splicing silencer N1 increase SMN levels and reduce disease severity in an animal model of spinal muscular atrophy. *Mol Ther* **20**: 119–126.
46. Pao, PW, Wee, KB, Yee, WC, Pramono, ZA and Dwipramono, ZA (2014). Dual masking of specific negative splicing regulatory elements resulted in maximal exon 7 inclusion of SMN2 gene. *Mol Ther* **22**: 854–861.
47. Hinderer, C, *et al.* (2014). Intrathecal gene therapy corrects CNS pathology in a feline model of mucopolysaccharidosis I. *Mol Ther*. 16 July 2014; doi:10.1038/mt.2014.135 (e-pub ahead of print).
48. Gray, SJ, Foti, SB, Schwartz, JW, Bachaboina, L, Taylor-Blake, B, Coleman, J *et al.* (2011). Optimizing promoters for recombinant adeno-associated virus-mediated gene expression in the peripheral and central nervous system using self-complementary vectors. *Hum Gene Ther* **22**: 1143–1153.
49. Mutsaers, CA, Wishart, TM, Lamont, DJ, Riessland, M, Schremel, J, Comley, LH *et al.* (2011). Reversible molecular pathology of skeletal muscle in spinal muscular atrophy. *Hum Mol Genet* **20**: 4334–4344.
50. Hayhurst, M, Wagner, AK, Cerletti, M, Wagers, AJ and Rubin, LL (2012). A cell-autonomous defect in skeletal muscle satellite cells expressing low levels of survival of motor neuron protein. *Dev Biol* **368**: 323–334.
51. Porensky, P.N. *et al.* (2012). A single administration of morpholino antisense oligomer rescues spinal muscular atrophy in mouse. *Hum Mol Genet* **21**: 1625–1638.
52. Glascock, J.J. *et al.* (2011). Delivery of therapeutic agents through intracerebroventricular (ICV) and intravenous (IV) injection in mice. *Journal of visualized experiments: JoVE*.